

Extraction of Metalloporphyrins Using Subcritical Toluene-Assisted Thermally Stable Ionic Liquid

Nor Faizatulfetri Salleh^{1,2}, Suzana Yusup³, Pradip Chandra Mandal⁴ and Muhammad Syafiq Hazwan Ruslan^{5,6*}

¹Department of Chemical Engineering, Universiti Teknologi PETRONAS, 32610 UTP, Seri Iskandar, Perak, Malaysia

²Centre of Research in Ionic Liquids, Institute of Contaminant Management, Universiti Teknologi PETRONAS, 32610 UTP, Seri Iskandar, Perak, Malaysia

³Fuel & Combustion Section, Generation Unit, Generation & Environment Department, TNBResearch, 43000 Kajang, Selangor, Malaysia

⁴Titas Gas Transmission and Distribution Co. Ltd., 105 Kuzi Nazrul Islam Avenue, Kawran Bazar, Dhaka, 1215, Bangladesh

⁵School of Chemical Engineering, College of Engineering, Universiti Teknologi MARA, 40450 UiTM, Shah Alam, Selangor, Malaysia

⁶Centre of Lipids Engineering and Applied Research, Ibnu Sina Institute of Scientific and Industrial Research, Universiti Teknologi Malaysia, 81310 UTM, Johor Bahru, Johor, Malaysia

ABSTRACT

Due to the depleting production of conventional petroleum, heavy oil is turned to as an alternative. However, the presence of trace nickel and vanadium in heavy oil poses problems for the refining process in producing lighter-end products. Such problems are its tendency to poison the catalyst, accumulate during distillation, and corrode the equipment. The objective of this work is to remove the metal porphyrins from model oil using the thermally stable ionic liquid 1-butyl-3-methylimidazolium octylsulfate, [BMIM][OS] assisted by subcritical toluene (above boiling point, 110.6°C and below a critical point, 318.6°C at 41.264 bar) in a novel attempt. The experiments were conducted at 150°C to 210°C under

a mixing time of 30 to 90 minutes while the pressure was monitored. Four metal porphyrins are used: nickel etioporphyrin, nickel tetraphenylporphyrin, vanadium oxide etioporphyrin, and vanadium oxide tetraphenylporphyrin. The results show that more than 40% of removal is achieved for all metal porphyrins, which shows great potential for further technological improvement. The Nuclear Magnetic

ARTICLE INFO

Article history:

Received: 11 June 2022

Accepted: 11 October 2022

Published: 13 June 2023

DOI: <https://doi.org/10.47836/pjst.31.4.22>

E-mail addresses:

faizatulfetri23@gmail.com (Nor Faizatulfetri Salleh)

suzana.yusup@tmb.com.my (Suzana Yusup)

pradipbd2002@yahoo.com (Pradip Chandra Mandal)

syafiqhazwan@uitm.edu.my (Muhammad Syafiq Hazwan Ruslan)

* Corresponding author

Resonance (NMR) shows that the ionic liquid did not decompose at the process temperature, which proves great stability. The extraction of metal porphyrins follows the second-order extraction model with an R² of more than 0.98.

Keywords: 1-butyl-3-methylimidazolium octylsulfate, heavy metals, heavy oil upgrading, metalloporphyrins, subcritical toluene

INTRODUCTION

The growth of population, transportation, and industry growth are the major drivers in increasing the demand for petroleum resources (Ali et al., 2018). The International Energy Agency reported that heavy oil production from Canada and Venezuela might reach 6 million barrels daily by 2030. Heavy oil can be defined as crude oil with the American Petroleum Institute (API) gravity of 10 to 20°, with high density and viscosity. Heavy oil fields are mostly in the United States, Russia, Canada, Venezuela, and the Middle East (Santos et al., 2014).

However, heavy oils contain a trace number of heavy metals, the most abundant being nickel and vanadium, which are highly troublesome heavy metals (Mandal et al., 2014). The content of vanadium can go up to 1200 ppm, while the content of nickel is up to 150 ppm (Agrawal & Wei, 1984). The presence of heavy metals can significantly impact the oil upgrading processes (Castañeda et al., 2014; Mandal & Alias, 2017; Mandal et al., 2011, 2012a, 2012b). It can cause the catalysts to be deactivated and poisoned, corrosion to the equipment, and raise concerns regarding toxic contents that may lead to environmental pollution.

Several porphyrin series are found in crude oil, with the most common type of porphyrin being etioporphyrin (ETIO) and deoxophylloerythroetio porphyrin (DPEP) (Zhao et al., 2015). Heavy metals in heavy oil are agglomerated in the asphaltene portion as porphyrin compounds referred to as metalloporphyrin (Rana et al., 2007). Treibs is reported to be the first to demonstrate the presence of metalloporphyrin in petroleum (Mandal et al., 2014). The general structure of porphyrins is shown in Figure 1.

Due to the drawbacks of conventional technologies, interest has grown in exploring unconventional methods to remove heavy metals from heavy oil. Examples of such methods are salting-out separation (Ameur & Husein, 2012), the use of zeolites as ion exchangers (Ikyereve et

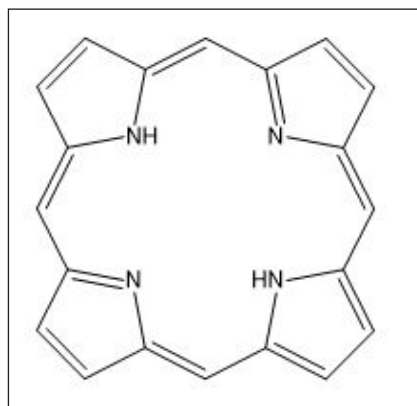


Figure 1. The general structure of porphyrin

al., 2014), electrochemical (Welter et al., 2009), microbial demetallization (Salehizadeh et al., 2007), microwave radiation (Wang et al., 2011), supercritical fluid application (Mandal et al., 2011, 2012a, 2012b; Manjare & Dhingra, 2019; Trucillo et al., 2019) and biosorption (Beni & Esmaili, 2020). Furthermore, there are a few methods explored to remove heavy metals from various environments, such as using ion exchange textiles (Elektorowicz & Muslat, 2008), via hydrochloric with alcohol extraction (Yuan et al., 2019) and integrated remediation processes (Selvi et al., 2019). However, these methods have their limitations.

Toluene is a good solvent for asphaltene (Painter et al., 2015), making it easier for metalloporphyrin extraction as it agglomerates in the asphaltene portion. Subcritical toluene is when toluene is above its boiling point (110.6°C) and below its critical point (318.6°C at 41.264 bar). The subcritical condition of toluene can generate a good environment for metal transfer during extraction. Furthermore, maintaining a subcritical condition is much easier than a supercritical condition due to the lower temperature and pressure requirement (Tavakoli & Yoshida, 2005).

Ionic liquids are salts that appear liquid at temperatures below 100°C and consist of cations and anions. Ionic liquids have seen applications for various purposes, such as CO₂ capture (Bara et al., 2010; Bates et al., 2002; Karadas et al., 2010; Ramdin et al., 2012), lubricants (Jiménez & Bermúdez, 2007; Qu et al., 2009), drug delivery agents (Dobler et al., 2013; Moniruzzaman et al., 2010; Monti et al., 2017), in biofuels (Fadeev & Meagher, 2001; Liu et al., 2012; Fauzi & Amin, 2012; Muhammad et al., 2015; Vancov et al., 2012), in the food industry (Hijo et al., 2016) and liquid-liquid extraction (Huddleston et al., 1998; Sun et al., 2012; Visser et al., 2001; Khaidzir et al., 2021). Researchers recognize Ionic liquids as a green solvent due to their unique properties, including their thermal stability, nonflammability, negligible vapor pressure, wide tunability for anions and cations, low volatility, and recyclability (Kumano et al., 2006; Sowmiah et al., 2009). In addition, ionic liquids have recently seen wide industrial use for applications in the separations, electroplating, reactions, and gas processing industry (Siriwardana, 2015).

Therefore, this study aims to extract the metalloporphyrin component in the heavy oil sample using ionic liquids under subcritical toluene solution as an alternative to heavy oil upgrading technology. Four metalloporphyrin components were selected: nickel etioporphyrin (NiEP), nickel tetraphenylporphyrin (NiTPP), vanadium oxide etioporphyrin (VOEP), vanadium oxide tetraphenylporphyrin (VOTPP), were selected for this study as the composition of these metals is significant in the heavy oil sample. A kinetic study on the extraction mechanism was also conducted to explain the fundamental behavior of the extraction process.

MATERIALS AND METHODS

Material and Apparatus

Nickel etioporphyrin (NiEP), nickel tetraphenylporphyrin (NiTPP), vanadium oxide etioporphyrin (VOEP), vanadium oxide tetraphenylporphyrin (VOTPP), 1-butyl-3-methylimidazolium octylsulfate, [BMIM][OS], and toluene were purchased from Avantis Laboratory Supply, Malaysia and were used without further treatment. The selection process was made using Conductor-like Screening Model for Realistic Solvents (COSMO-RS) software, where the prediction of the selectivity, capacity, and performance index toward the 4 metalloporphyrin metals.

All metalloporphyrin structures were drawn and optimized in the TURBOMOLE program using its quantum chemical calculation. Functional BP86 with triple- ζ valence polarized (TZVP) basis set, a function in density functional theory (DFT), was used to optimize the metalloporphyrin structure. The optimized structures were then imported to the COSMO-RS software for activity coefficient estimation. Cations and anions for the ionic liquids were called from the existing COSMO-RS library. The activity coefficient in infinite dilution was used to estimate the selectivity and capacity of ionic liquid towards metalloporphyrin. Equations 1 to 3 shows the equation used to calculate the tested ionic liquid's capacity, selectivity, and performance index

$$C^{\infty} = \left(\frac{1}{\gamma_1^{\infty}} \right)^{IL\ phase} \quad [1]$$

$$S_{12}^{\infty} = \frac{\gamma_2^{\infty}}{\gamma_1^{\infty}} \quad [2]$$

$$PI = C^{\infty} \times S^{\infty} = \left(\frac{\gamma_2^{\infty}}{(\gamma_1^{\infty})^2} \right)^{IL\ phase} \quad [3]$$

Whereby C^{∞} is the capacity at infinite dilution, γ_1^{∞} is the activity coefficient of metalloporphyrin at infinite dilution in ionic liquid, γ_2^{∞} is the activity of toluene at infinite dilution in ionic liquid, S_{12}^{∞} is the selectivity of metalloporphyrin and toluene towards the ionic liquid in infinite dilution, and PI is the performance indicator.

The 12 shortlisted ionic liquids are 1-ethyl-3-methylimidazolium octylsulfate [EMIM][OS], 1-ethyl-3-methylimidazolium bis((trifluoromethyl)sulfonyl)imide [EMIM][NTf2], 1-ethyl-3-methylimidazolium hydrogensulfate [EMIM][HS], 1-ethyl-3-methylimidazolium methanesulfonate [EMIM][MS], 1-butyl-3-methylimidazolium octylsulfate [BMIM][OS], 1-butyl-3-methylimidazolium bis((trifluoromethyl)sulfonyl)imide [BMIM][NTf2], 1-butyl-3-methylimidazolium hydrogensulfate [BMIM][HS], 1-butyl-3-methylimidazolium methanesulfonate [BMIM][MS], tetrabutylphosphonium octylsulfate

[TBP][OS], tetrabutylphosphonium bis((trifluoromethyl)sulfonyl)imide [TBP][NTf₂], tetrabutylphosphonium hydrogensulfate [TBP][HS], and tetrabutylphosphonium methanesulfonate [TBP][MS].

Based on the screening process, [TBP]⁺ cation shows the best performance index, followed by [BMIM]⁺ and [EMIM]⁺. However, [TBP]⁺ has low selectivity towards the metalloporphyrin complex. Moreover, it is unstable due to the formation of an unwanted by-product, phosphine oxide, in the presence of oxygen.

Meanwhile, for the anion screening, [OS]⁻ and [NTf₂]⁻ show potential since both anions show good performance index compared to [HS]⁻ and [MS]⁻. However, a study has shown that [OS] was reasonably non-toxic, has an acceptable biodegradability, and is a cheaper option compared to [NTf₂]⁻ (Dávila et al., 2007; Davis & Fox, 2003). Therefore, [BMIM][OS] was selected as the extractant.

The experiments were conducted in a 100 mL autoclave-stirred reactor from Amar Equipment Pvt. Ltd., India. The reactor was manufactured from stainless steel, with a stirrer and pressure gauge attached, and was designed for temperatures of up to 500°C and pressures up to 20 MPa.

Generating Calibration Curve

Five standard solutions of model oil ranging from 20 to 100 ppm were prepared. The samples were analyzed using UV-Visible Spectrophotometer 1800 model from Shimadzu Scientific Instrument, US, and were scanned at 200 to 700 nm wavelengths. The analysis used 12.5 × 12.5 × 45 mm quartz cuvettes, and toluene was used as a reference. The concentration of porphyrin was computed by applying the Lambert-Beer Law.

Experiment Procedure

A stock solution of model oil was first prepared. Then, 0.015 g of metal porphyrin was dissolved in 50 mL of toluene at 30°C with continuous stirring at 150 rpm. Next, 150 mL of toluene was added thrice over a certain period. After the metal porphyrin had completely dissolved, the mixture was transferred into a 250 mL volumetric flask, and toluene was added till the calibration mark.

Metal porphyrins were extracted by loading 20 mL of model oil and 2 mL of [BMIM][OS] into the autoclave reactor. Then, the mixture was heated up at temperatures of 150 to 210°C under mixing times of 30 to 90 minutes, with intervals of 30°C and 30 minutes, respectively. Meanwhile, the pressure throughout the extraction process was monitored. Next, the mixture was cooled down at room temperature and transferred into a separating funnel. In the 2 layers observed to form, the bottom layer was the extract, and the upper layer was the raffinate. After that, the two layers were separated and sent for analysis for further examination.

The percentage of metal porphyrin extraction was calculated using the following Equation 4:

$$\text{Removal (\%)} = [(C_i - C_f)/C_i] \times 100 \quad [4]$$

where C_i is the initial concentration of model oil, and C_f is the final concentration of the model oil.

Analysis

UV-Visible (UV-Vis spectrophotometer 1800 model, Thermo Fisher Scientific Inc., US) and Fourier Transform Infrared Spectroscopy (FTIR) coupled with diamond Attenuated Total Reflectance (Nicolet iS5, Thermo Fisher Scientific Inc., US) were used for the upper layer which contains model oil. The wavelength of FTIR used ranges from 4000 to 400 cm^{-1} with 16 cycles of scanning. Meanwhile, FTIR and Nuclear Magnetic Resonance (NMR) (Bruker Advance III 500 MHz, Bruker Corporation, US) was used to analyze the bottom layer, which contains [BMIM][OS] and the metal porphyrin. The NMR analysis was done at ambient temperature, and dimethyl sulfoxide (DMSO) was used as a solvent.

Kinetic Study

A second-order extraction model was used to determine the mechanism of the metal porphyrins extraction. The model was calculated using the following linear Equation 5:

$$t/C_t = [1/(k_2 C_s^2)] + (t/C_s) \quad [5]$$

where C_s and C_t are concentrations of metal porphyrin at saturation (mg/L) and metal porphyrin at any extraction time (mg/L), respectively, k_2 was the rate coefficient of second-order extraction (min^{-1}), and t was the extraction time (min). C_s and k_2 were obtained from the slope and intercept of the t/C_t vs. t graph.

RESULTS AND DISCUSSION

Effect of Temperature

Subcritical Condition. The experiment was carried out to study the effect of temperature on metalloporphyrin extraction using subcritical toluene-assisted ionic liquid. The experiment was done at 150°C (9 bar), 180°C (10 bar), and 210°C (11 bar). The ionic liquid used in this work is [BMIM][OS]. Four types of metalloporphyrin are studied in this work: NiEP, NiTPP, VOEP, and VOTPP. The results obtained are shown in Figures 2 to 4.

Figure 2 demonstrates the extraction results for NiEP. It was observed that the temperature and mixing time affected the extraction of NiEP differently. The removal (%) indicates the efficiency of metalloporphyrin extraction using subcritical toluene-assisted

thermally stable ionic liquid. As the mixing time increased, the extraction of NiEP increased. It is due to the longer contact time between [BMIM][OS] and the metal complexes, resulting in more metal complexes being extracted. However, the removal of NiEP increased from $30\% \pm 0.9$ to $60\% \pm 1.1$ when the temperature was raised from 150°C to 180°C . As rising temperatures could reduce the viscosity of the extractant, this also leads to a higher solubility of the metal complexes. The solubility increased from $265 \mu\text{g NiEP/g [BMIM][OS]}$ at 150°C to $399 \mu\text{g NiEP/g [BMIM][OS]}$ at 180°C . Then, the extraction of NiEP decreased by $13\% \pm 0.75$ when the temperature reached 210°C . The maximum extraction of NiEP is achieved at 60% , under a temperature of 180°C and mixing time of 90 minutes. The most significant parameter is temperature. However, the deep knowledge of the fate of metal in this reaction remains unclear. Mandal et al. (2012b) stated that the fate of the central metal group in the reaction was not explained.

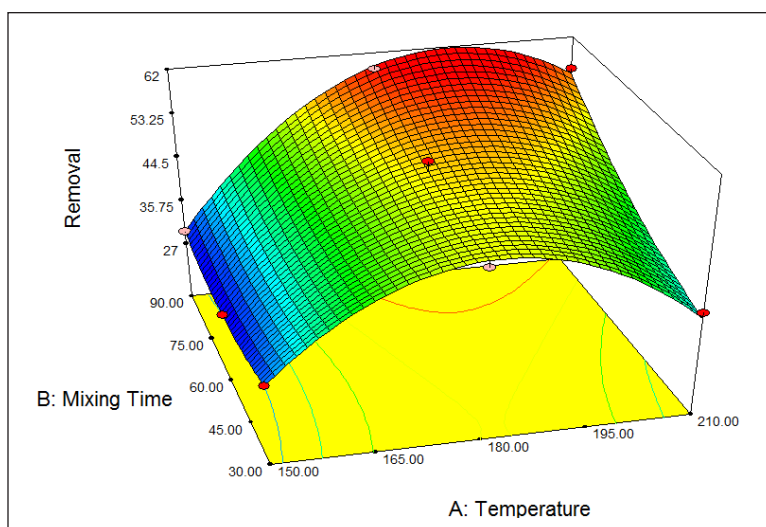


Figure 2. Effect of mixing time and temperature on the removal percentage of NiEP (%)

Meanwhile, Figure 3 illustrates the extraction results for NiTPP. The surface plot shows that the removal decreased by 10% (from $50\% \pm 0.4$ to $40\% \pm 0.9$) when the temperature increased from 150°C to 180°C . Then, it increased up to $60\% \pm 0.9$ of extraction when the temperature reached 210°C , except for the case of 90 minutes of mixing time where the extraction was reduced by as much as $20\% \pm 0.6$ as the temperature increased. The highest extraction of NiTPP was accomplished at a temperature of 150°C and a mixing time of 90 minutes, where [BMIM][OS] could extract approximately 70% of NiTPP. Mandal et al. (2011) reported that the fate of a central metal group of NiTPP under supercritical conditions remains uncertain. This sentiment was supported by the work of Bonné et al. (2001), which also stated that the fate of the central metal group under non-catalytic demetallization remained obscure.

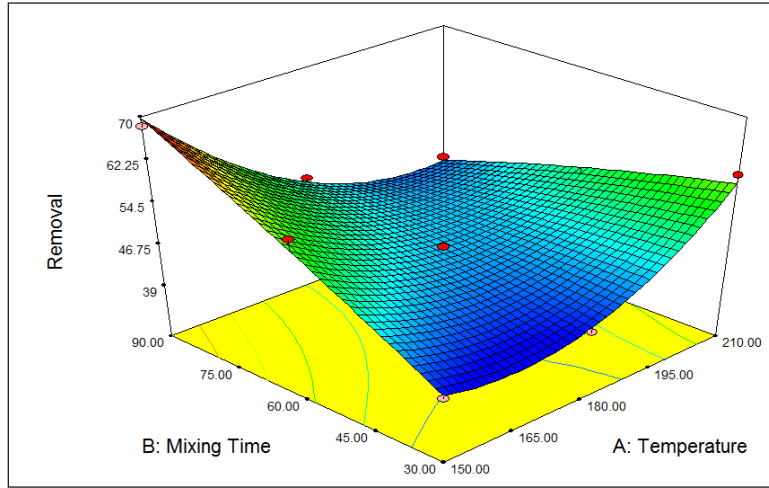


Figure 3. Effect of mixing time and temperature on the removal percentage of NiTPP (%)

Similarly, the extraction of NiEP was slightly increased when extraction time increased from 30 minutes to 60 minutes. Then, it increased by 10% when the extraction time increased to 90 minutes. These results indicate that the longer the extraction time, the longer the extractant contacted NiEP, thus increasing the NiEP extraction. On the other hand, the NiTPP extraction was increased as extraction time increased except for a temperature of 210°C, where the NiTPP was slightly decreased.

Figure 4 shows the effect of temperature on VOEP extraction. As the temperature increased from 150°C to 180°C, the extraction drastically increased by almost 20% (from 30% ± 0.5 to 50% ± 0.9). It then increased slightly further by 7% (57% ± 0.8) when the

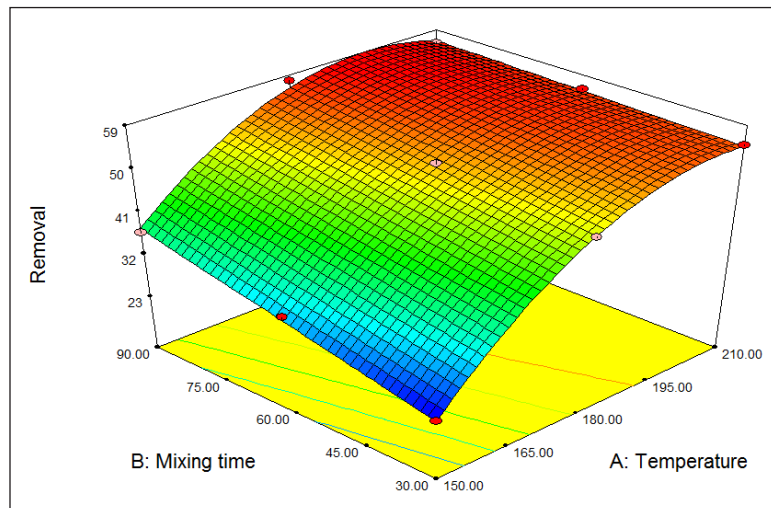


Figure 4. Effect of mixing time and temperature on the removal percentage of VOEP (%)

temperature was extended to 210°C. It is due to the reduction of the viscosity of [BMIM][OS], which increases the contact surface, thus leading to higher extraction of VOEP. Besides, the reduction in viscosity of [BMIM][OS] also leads to an increase in metal transfer in ionic liquid (Germani et al., 2007). Consequently, VOEP extraction was increased as temperature increased. However, when the mixing time is increased from 30 minutes to 90 minutes, the removal of VOEP increases slightly. Mandal et al. (2012a) studied the removal of VOEP using supercritical water. The results showed that the conversion rate of VOEP showed a significant increase, followed by a slight increase when the temperature was raised to 490°C. It is stated that the reversible reaction took place and reached equilibrium within a reaction time of 90 minutes.

Figure 5 reveals the extraction of VOTPP using subcritical toluene assisted [BMIM][OS]. Based on the surface plot, the VOTPP extraction was reduced by 10 to 13% extraction (from $30\% \pm 0.5$ to approximately $20\% \pm 0.5$) when the temperature was increased from 150°C to 180°C. Then, the extraction was increased by 5 to 10% (approximately $30\% \pm 0.8$) when the temperature extended to 210°C. However, the prediction of the structure of porphyrin conformation under several environments was challenging because only low amounts of energy were used to change the conformation of porphyrin structure. A deep understanding of detailed porphyrin conformation in solution remained obscure due to inadequate knowledge of solvent-porphyrin interactions (Fleischer, 1970).

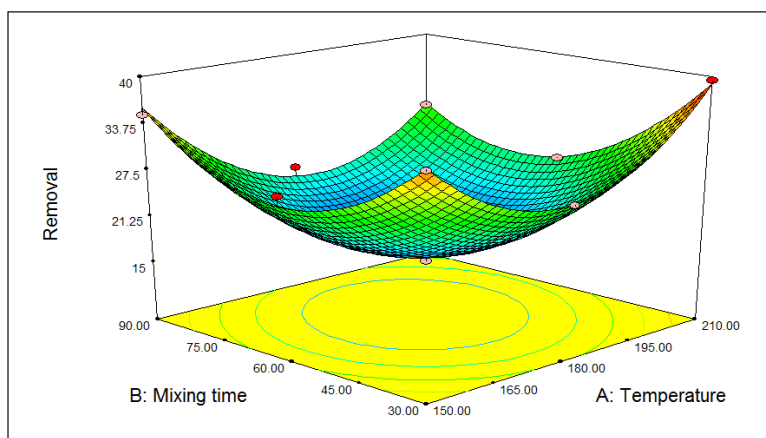


Figure 5. Effect of mixing time and temperature on the removal percentage of VOTPP (%)

Likewise, the VOEP extraction was significantly increased when extraction time increased from 30 minutes to 90 minutes. However, VOEP extraction slightly inclined when it operated at 210°C. On the other hand, the VOTPP extraction declined when the extraction time increased from 30 minutes to 60 minutes, then increased when the extraction time was extended to 90 minutes.

Comparison of Metalloporphyrin Removal at Normal Condition and Subcritical Condition. Experiments were done to compare the performance of toluene-assisted [BMIM][OS] on metalloporphyrin extraction at normal conditions (below boiling point, 90°C) and subcritical condition (210°C). The results obtained with the error bar are shown in Figure 6. It was observed that subcritical toluene had improved in assisting [BMIM][OS] to extract the metalloporphyrin. Nickel porphyrin extraction was higher than vanadium porphyrin extraction. It is because nickel porphyrin is more stable with regard to demetallization due to the shorter distance of the Ni-Nitrogen bond (Fleischer, 1970). The extraction of nickel porphyrin increased from 23% to 36% and from 39% to 60% for NiEP and NiTPP, respectively. Meanwhile, the extraction of vanadium porphyrin increased from 40% to 55% and from 23% to 40% for VOEP and VOTPP, correspondingly.

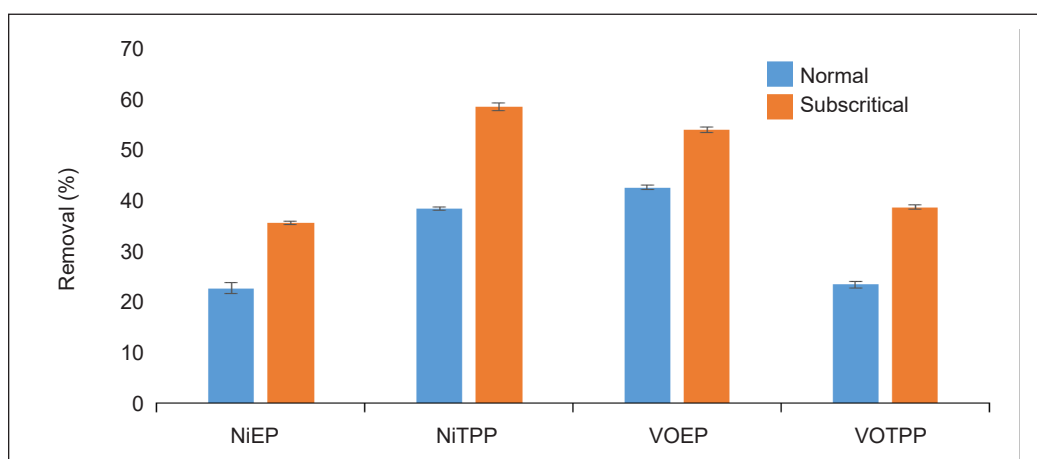


Figure 6. Comparison of metalloporphyrin extraction at normal conditions and subcritical condition

Analysis

Fourier Transform Infrared Spectroscopy (FTIR). The functional groups of [BMIM][OS] were studied regarding their structural changes before and after extraction. Therefore, FTIR analysis was carried out. Figures 7 to 10 illustrate the spectra of pure [BMIM][OS], pure toluene, [BMIM][OS] after extraction, and pure metal porphyrins (NiEP, NiTPP, VOEP, and VOTPP). It was observed that spectra bands above 3000 cm^{-1} represented the C-H at imidazolium rings of [BMIM][OS], while bands of 2927 to 2853 cm^{-1} represented CH_2 of alkyl chains. Wavelengths between 1466.05 to 1457 cm^{-1} show the symmetry and asymmetry stretching of C-H scissoring vibrations of CH_3 -moiety. C-C stretching vibrations were observed at a wavelength of 1572 cm^{-1} .

In addition, the spectra bands at 1379 cm^{-1} refer to the C=C stretching vibrations. The spectra peaks of C-N stretching shifted from the wavelength of 1217 cm^{-1} to 1219-1210 cm^{-1} . On the other hand, spectra bands at 1057 cm^{-1} and 982 cm^{-1} correspond to C-O and

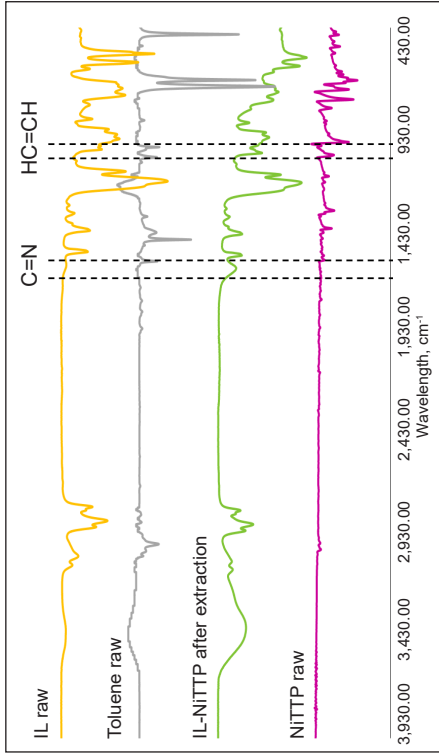


Figure 8. IR spectra of pure [BMIM][OS], pure toluene, [BMIM][OS] after extraction and pure NiTPP

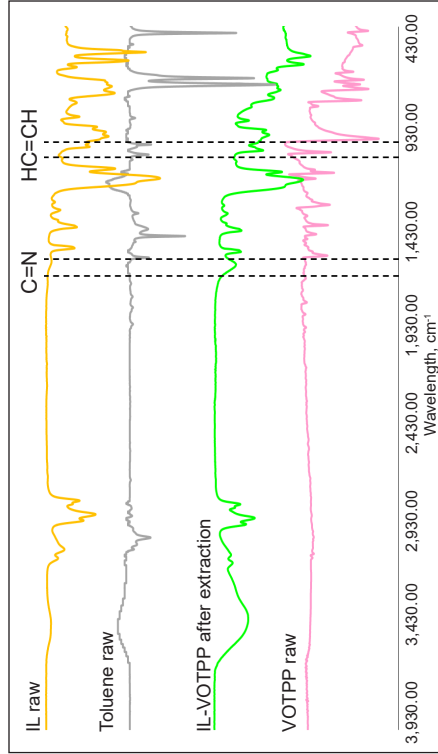


Figure 10. IR spectra of pure [BMIM][OS], pure toluene, [BMIM][OS] after extraction and pure VOTPP

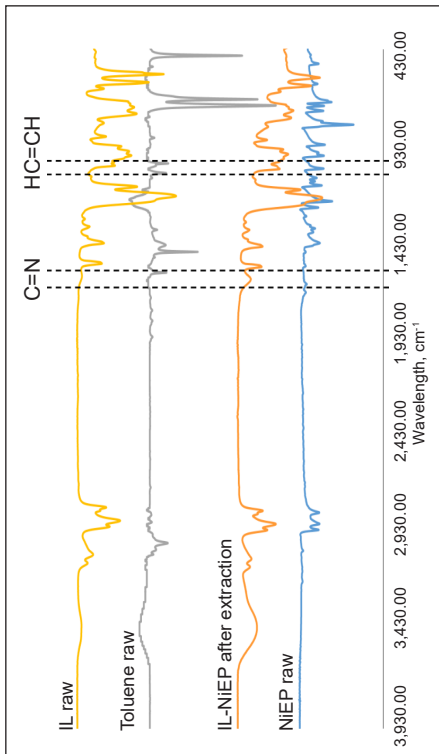


Figure 7. IR spectra of pure [BMIM][OS], pure toluene, [BMIM][OS] after extraction and pure NiEP

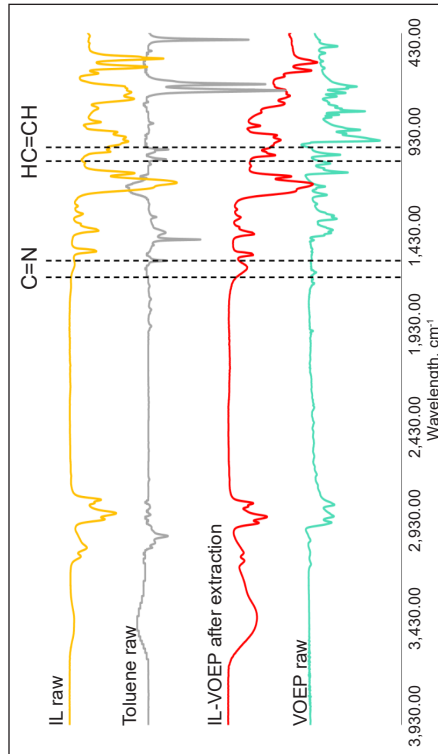


Figure 9. IR spectra of pure [BMIM][OS], pure toluene, [BMIM][OS] after extraction and pure VOEP

S-O stretching vibrations, respectively, while the spectra at 905 cm^{-1} represent aromatic C-H bending vibrations. However, new peaks were detected at wavelengths of 1637 and 1060 cm^{-1} . These peaks represent C=N and HC=CH of metal porphyrins in [BMIM][OS] after the extraction, respectively, indicating that the [BMIM][OS] was able to extract metal porphyrins successfully.

Figure 11 compares IR spectra of pure [BMIM][OS], pure toluene, and NiEP solution after extraction. It is noted that no new peaks were found in the NiEP solution after the extraction, indicating that the [BMIM][OS] does not dissolve into the model oil solution while extracting the metalloporphyrins. The same result was obtained for NiTPP, VOEP, and VOTPP solutions. It shows that the ionic liquid is suitable for extraction, as the extracting agent is immiscible to the solution containing the solute to be extracted.

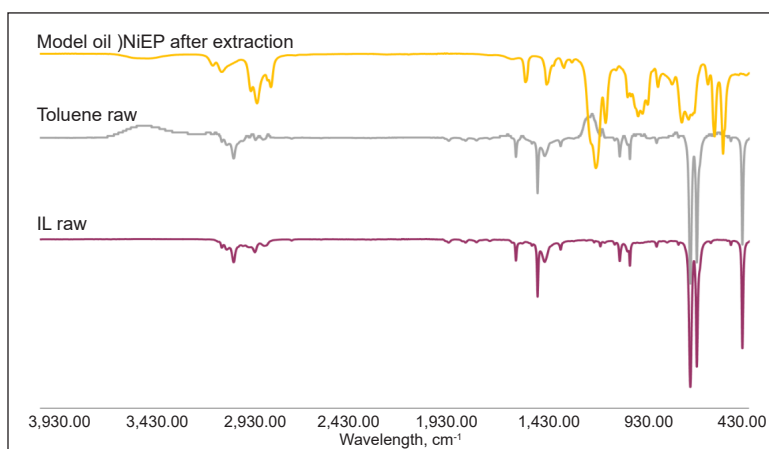


Figure 11. IR spectra of pure [BMIM][OS], pure toluene, and NiEP solution after extraction

Nuclear Magnetic Resonance (NMR). Initially, [BMIM][OS] was thermally stable at the operating temperature used in this work. A study of the structural decomposition of [BMIM][OS] was carried out using NMR analysis to confirm this. [BMIM][OS] has the molecular formula of $\text{C}_{16}\text{H}_{32}\text{N}_2\text{O}_4\text{S}$. Figure 12 demonstrates the NMR spectrum of [BMIM][OS] before and after the extraction of metalloporphyrin, where dimethyl sulfoxide (DMSO) was used as a solvent.

The ^1H NMR peaks of DMSO were 2.5 and 3.5 ppm. Meanwhile, for [BMIM][OS], ^1H NMR (δ/ppm): 9.157 (s, 1H), 7.79 and 7.72 (two s, $2 \times 1\text{H}$), 4.19 to 4.16 (t, 2H), 3.867 (s, 3H), 3.717 and 3.69 (t, 2H), 1.802 to 1.749 (m, 2H), 1.5 to 1.459 (m, 2H), 1.287 to 1.249 (m, 12H), 0.91 (t, 3H) and 0.9 (t, 3H). The comparison of peaks found in Figure 12 indicates that the structure of [BMIM][OS] does not decompose during the metalloporphyrin extraction process, therefore confirming the thermal stability of [BMIM][OS] for the application within this work. Hence, [BMIM][OS] can be recovered for further experiments, though the actual recoverable amount of [BMIM][OS] is not further studied

in this work. However, ^1H NMR cannot detect the extracted metalloporphyrin in [BMIM][OS] due to the limitations of the equipment.

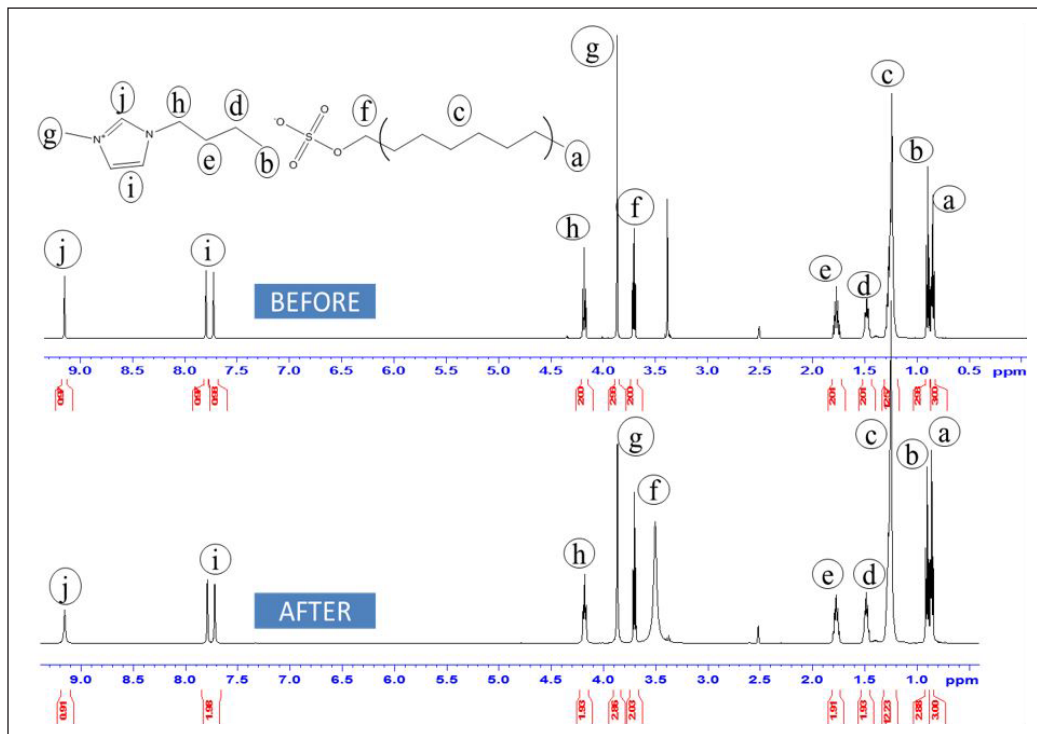


Figure 12. ^1H NMR of [BMIM][OS] before and after the extraction

Kinetic Study

The mechanism of metalloporphyrin extraction using subcritical toluene-assisted thermally stable [BMIM][OS] was studied by applying a second-order extraction model. Several graphs were plotted using Equation 5 for all the different cases of metalloporphyrin extraction (Figures 13 to 16). Based on the linear graph, it was concluded that the second-order model accurately described the experimental data of metalloporphyrin extraction, as the data fitted closely in a straight line.

The value of C_s and k were obtained from the slope and intercept of the linear graphs in Figures 13 to 16, and all values found in the kinetic study are tabulated in Table 1. The R^2 of the second-order models was higher than 0.98, further supporting that the model fitted the experimental data very well. The C_s calculated using the second-order model are close to those obtained from the experiment. The value of k increases as the temperature is raised from 150°C to 180°C, and it decreases when the temperature rise is prolonged until it reaches 210°C, except for NiEP. The main finding here is that the extraction of metalloporphyrin is faster at temperatures between 150°C to 180°C.

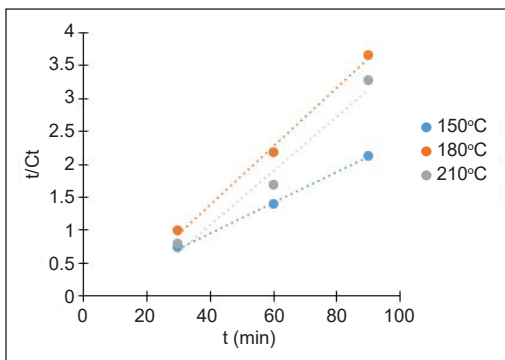


Figure 13. Linear graph of extraction second-order model for NiEP

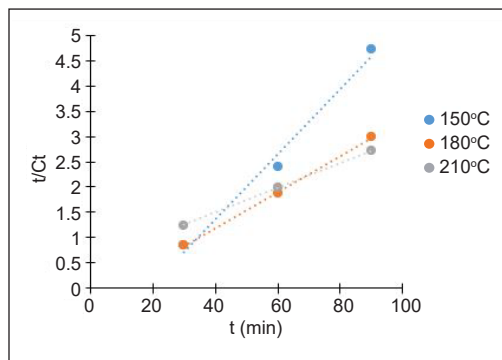


Figure 14. Linear graph of extraction second-order model for NiTPP

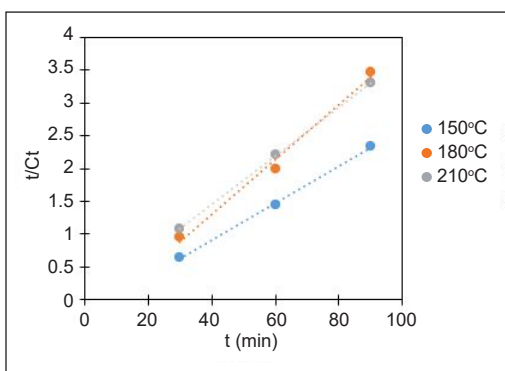


Figure 15. Linear graph of extraction second-order model for VOEP

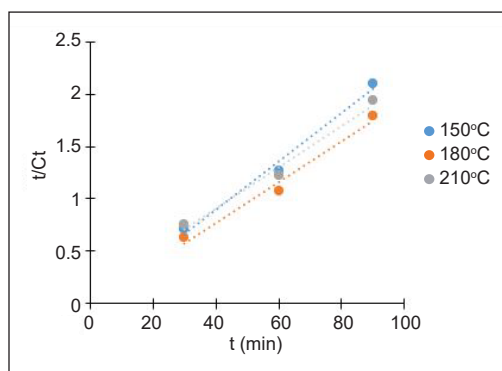


Figure 16. Linear graph of extraction second-order model for VOTPP

The extraction is kinetic and was compared with the pseudo-first-order kinetic model ($\ln(C_s/(C_s - C_t)) = k_1 t$). Based on the tabulated data in Table 1, the pseudo-first-order model is not in good agreement with an average R^2 value of 0.69. Compared with the second-order kinetic model R^2 value of 0.99, the second-order model shows a better fit. The high R^2 obtained indicates that the sorption process of extraction of metalloporphyrin is based on chemisorption. The results demonstrate good agreement with the FTIR spectra gained, where new peaks were found in [BMIM][OS] spectra after the extraction, showing that the extraction occurred through chemical interactions. Besides, subcritical conditions' pressure resulted in chemisorption as this sorption required high pressure. However, a deep understanding of the underlying mechanism of metalloporphyrins removal using subcritical toluene-assisted thermally stable [BMIM][OS] is still obscure.

Previous work done by Mandal et al. (2012a, 2012b) reported that the disappearance of NiEP and VOEP under supercritical water followed a first-order model. Similar results were also reported by Chen and Massoth, where the disappearance rate of nickel porphyrins

Table 1
Data comparison of the pseudo-first-order and second-order kinetic model

Metal Porphyrin	T (°C)	Pseudo First-order model				Second order model				
		C _{S,exp} (mg/L)	C _{S,cal} (mg/L)	z (min ⁻¹)	R ²	C _{S,exp} (mg/L)	C _{S,cal} (mg/L)	k (L/(mg·min))	h (mg/L·min)	R ²
NiEP	150	42.31	41.002	0.000461	0.3274	42.31	42.92	0.030499	56.18	0.9989
	180	24.65	33.81	0.003455	0.9993	24.65	22.52	0.005038	2.56	0.9964
	210	27.59	46.47	0.005527	0.8928	27.59	24.21	0.002995	1.76	0.9744
NiTPP	150	19.04	47.6	0.010364	0.996	19.04	15.48	0.003416	0.82	0.9864
	180	30.11	37.95	0.002533	0.9832	30.11	28.09	0.005421	4.28	0.9994
	210	33.15	21.03	0.005297	0.9519	33.15	40.82	0.001173	1.96	0.9864
VOEP	150	38.46	50.71	0.003224	0.9942	38.46	35.46	0.00365	4.59	0.9986
	180	25.9	35.56	0.003455	0.9271	25.9	27.03	0.051082	37.31	0.9999
	210	27.29	27.98	0.00023	0.6931	27.29	23.75	0.004575	2.58	0.9904
VOTPP	150	42.92	43.9	0.000138	0.0042	42.92	43.1	0.014626	27.17	0.9876
	180	50.12	49.25	0.000691	0.0672	50.12	51.28	0.04321	113.64	0.9814
	210	46.44	38.72	0.002533	0.4919	46.44	50.51	0.003374	8.61	0.9855

*C_{S,exp} and C_{S,cal} represent the concentration of metalloporphyrin extracted from experimental work and calculation, respectively.

using CoMo/Al₂O₃ catalyst followed a first-order kinetic model behavior (Chen & Massoth, 1988). Tangentially, the disappearance rate of nickel porphyrins using a CoO-MoO₃/Al₂O₃ catalyst was reported to follow a half-order kinetic model (Hung & Wei, 1980).

CONCLUSION

The presence of heavy metals in heavy oils presents significant challenges to current upgrading technologies, necessitating the development of pretreatment methods to remove these heavy metals. Using subcritical toluene-assisted thermally stable ionic liquid, [BMIM][OS] shows remarkable results on metalloporphyrin extraction where approximately 60%, 68%, 58%, and 40% removal is achieved for NiEP, NiTPP, VOEP, and VOTPP respectively. The FTIR spectra supported the results, where new peaks were found in [BMIM][OS], representing the metalloporphyrins' structure. Besides, the NMR spectrum shows [BMIM][OS] does not decompose during the extraction process, indicating this IL is thermally stable at the operational condition. Furthermore, the extraction has proven to follow a second-order model, which reveals that the process involves chemisorption. Therefore, the extraction efficiency obtained in this work indicates that subcritical toluene-assisted thermally stable ionic liquid had the potential for metalloporphyrin removal. For a future perspective, it is suggested that a continuous process is required to study the extraction of metalloporphyrin, as this work was done by processing per batch. Furthermore, it is proposed to investigate the recovery of ionic liquid with the highest extraction of metalloporphyrin. Besides, it is recommended to examine techno-economic analysis to study the feasibility of implementing this technology on a larger scale.

ACKNOWLEDGMENTS

The authors thank the Centre of Research in Ionic Liquids (CORIL), Universiti Teknologi PETRONAS (UTP), Perak, Malaysia, for providing a conducive environment and necessary facilities for this research work. This research was funded by Yayasan Universiti Teknologi PETRONAS (YUTP) (Cost center: 0153AA-E33) and (Cost center: 015LC0-257).

REFERENCES

- Agrawal, R., & Wei, J. (1984). Hydrodemetalation of nickel and vanadium porphyrins. 1. Intrinsic kinetics. *Industrial & Engineering Chemistry Process Design and Development*, 23(3), 505-514. <https://doi.org/10.1021/i200026a017>
- Ali, S. A., Suboyin, A., & Haj, H. B. (2018). Unconventional and conventional oil production impacts on oil price - Lessons learnt with glance to the future. *Journal of Global Economics*, 06(1), Article 1000286. <https://doi.org/10.4172/2375-4389.1000286>
- Ameur, Z. O., & Husein, M. M. (2012). Salting-out induced aggregation for selective separation of vanadyl-oxide tetraphenyl-porphyrin from heavy oil. *Energy & Fuels*, 26(7), 4420-4425. <https://doi.org/10.1021/ef300482h>

- Bara, J. E., Camper, D. E., Gin, D. L., & Noble, R. D. (2010). Room-temperature ionic liquids and composite materials: Platform technologies for CO₂ capture. *Accounts of Chemical Research*, 43(1), 152-159. <https://doi.org/10.1021/ar9001747>
- Bates, E. D., Mayton, R. D., Ntai, I., & Davis, J. H. (2002). CO₂ capture by a task-specific ionic liquid. *Journal of the American Chemical Society*, 124(6), 926-927. <https://doi.org/10.1021/ja017593d>
- Beni, A. A., & Esmaceli, A. (2020). Biosorption, an efficient method for removing heavy metals from industrial effluents: A review. *Environmental Technology & Innovation*, 17, Article 100503. <https://doi.org/10.1016/j.eti.2019.100503>
- Bonné, R. L. C., van Steenderen, P., & Moulijn, J. A. (2001). Hydrogenation of nickel and vanadyl tetraphenylporphyrin in absence of a catalyst: A kinetic study. *Applied Catalysis A: General*, 206(2), 171-181. [https://doi.org/10.1016/S0926-860X\(00\)00587-1](https://doi.org/10.1016/S0926-860X(00)00587-1)
- Castañeda, L. C., Muñoz, J. A. D., & Ancheyta, J. (2014). Current situation of emerging technologies for upgrading of heavy oils. *Catalysis Today*, 220-222, 248-273. <https://doi.org/10.1016/j.cattod.2013.05.016>
- Chen, H. J., & Massoth, F. E. (1988). Hydrodemetalation of vanadium and nickel porphyrins over sulfided cobalt-molybdenum/alumina catalyst. *Industrial & Engineering Chemistry Research*, 27(9), 1629-1639. <https://doi.org/10.1021/ie00081a012>
- Dávila, M. J., Aparicio, S., Alcalde, R., García, B., and Leal, J. M. (2007). On the properties of 1-butyl-3-methylimidazolium octylsulfate ionic liquid. *Green Chemistry*, 9(3), 221-232. <https://doi.org/10.1039/B612177B>
- Davis, Jr., J. H. & Fox, P. A. (2003). From curiosities to commodities: Ionic liquids begin the transition. *Chemical Communications*, 11, 1209-1212, <https://doi.org/10.1039/b212788a>.
- Dobler, D., Schmidts, T., Klingenhöfer, I., & Runkel, F. (2013). Ionic liquids as ingredients in topical drug delivery systems. *International Journal of Pharmaceutics*, 441(1-2), 620-627. <https://doi.org/10.1016/j.ijpharm.2012.10.035>
- Elektorowicz, M., & Muslat, Z. (2008). Removal of heavy metals from oil sludge using ion exchange textiles. *Environmental Technology*, 29(4), 393-399. <https://doi.org/10.1080/09593330801984290>
- Fadeev, A. G., & Meagher, M. M. (2001). Opportunities for ionic liquids in recovery of biofuels. *Chemical Communications*, 3, 295-296. <https://doi.org/10.1039/b006102f>
- Fauzi, A. H. M., & Amin, N. A. S. (2012). An overview of ionic liquids as solvents in biodiesel synthesis. *Renewable and Sustainable Energy Reviews*, 16(8), 5770-5786. <https://doi.org/10.1016/j.rser.2012.06.022>
- Fleischer, E. B. (1970). Structure of porphyrins and metalloporphyrins. *Accounts of Chemical Research*, 3(3), 105-112. <https://doi.org/10.1021/ar50027a004>
- Germani, R., Mancini, M., Savelli, G., & Spreti, N. (2007). Mercury extraction by ionic liquids: Temperature and alkyl chain length effect. *Tetrahedron Letters*, 48(10), 1767-1769. <https://doi.org/10.1016/j.tetlet.2007.01.038>
- Hijo, A. A. C. T., Maximo, G. J., Costa, M. C., Batista, E. A. C., & Meirelles, A. J. A. (2016). Applications of ionic liquids in the food and bioproducts industries. *ACS Sustainable Chemistry & Engineering*, 4(10), 5347-5369. <https://doi.org/10.1021/acssuschemeng.6b00560>

- Huddleston, J. G., Willauer, H. D., Swatoski, R. P., Visser, A. E., & Rogers, R. D. (1998). Room temperature ionic liquids as novel media for 'clean' liquid-liquid extraction. *Chemical Communications*, 16, 1765-1766. <https://doi.org/10.1039/A803999B>
- Hung, C. W., & Wei, J. (1980). The kinetics of porphyrin hydrodemetallation. 1. Nickel compounds. *Industrial & Engineering Chemistry Process Design and Development*, 19(2), 250-257. <https://doi.org/10.1021/i260074a009>
- Ikyereve, R. E., Nwankwo, C., & Mohammed, A. (2014). Selective removal of metal ions from crude oil using synthetic zeolites. *International Journal of Scientific and Research Publications*, 4(5), 411-413.
- Jiménez, A. E., & Bermúdez, M. D. (2007). Ionic liquids as lubricants for steel-aluminum contacts at low and elevated temperatures. *Tribology Letters*, 26(1), 53-60. <https://doi.org/10.1007/s11249-006-9182-9>
- Karadas, F., Atilhan, M., & Aparicio, S. (2010). Review on the use of ionic liquids (ILs) as alternative fluids for CO₂ capture and natural gas sweetening. *Energy & Fuels*, 24(11), 5817-5828. <https://doi.org/10.1021/ef1011337>
- Khaidzir, S., Masri A. N., Ruslan, M. S. H., & Mutalib, M. I. A. (2021). Ultrasonic-assisted technique as a novel method for removal of naphthenic acid from model oil using piperidinium-based ionic liquids. *ACS Omega*, 6(14), 9629-9637.
- Kumano, M., Yabutani, T., Motonaka, J., & Mishima, Y. (2006). Recovery and extraction of heavy metal ions using ionic liquid as green solvent. *International Journal of Modern Physics B*, 20(25n27), 4051-4056. <https://doi.org/10.1142/S0217979206040842>
- Liu, C. Z., Wang, F., Stiles, A. R., & Guo, C. (2012). Ionic liquids for biofuel production: Opportunities and challenges. *Applied Energy*, 92, 406-414. <https://doi.org/10.1016/j.apenergy.2011.11.031>
- Mandal, P., & Alias, M. A. (2017). Investigation of asphaltene under subcritical water treatment. *International Journal of Materials, Mechanics and Manufacturing*, 5(1), 11-15. <https://doi.org/10.18178/ijmmm.2017.5.1.279>
- Mandal, P. C., Goto, M., & Sasaki, M. (2014). Removal of nickel and vanadium from heavy oils using supercritical water. *Journal of the Japan Petroleum Institute*, 57(1), 18-28. <https://doi.org/10.1627/jpi.57.18>
- Mandal, P. C., Wahyudiono, Sasaki, M., & Goto, M. (2011). Nickel removal from nickel-5,10,15,20-tetraphenylporphine using supercritical water in absence of catalyst: A basic study. *Journal of Hazardous Materials*, 187(1-3), 600-603. <https://doi.org/10.1016/j.jhazmat.2011.01.059>
- Mandal, P. C., Wahyudiono, Sasaki, M., & Goto, M. (2012a). Non-catalytic vanadium removal from vanadyl etioporphyrin (VO-EP) using a mixed solvent of supercritical water and toluene: A kinetic study. *Fuel*, 92(1), 288-294. <https://doi.org/10.1016/j.fuel.2011.07.002>
- Mandal, P. C., Wahyudiono, Sasaki, M., & Goto, M. (2012b). Nickel removal from nickel etioporphyrin (Ni-EP) using supercritical water in the absence of catalyst. *Fuel Processing Technology*, 104, 67-72. <https://doi.org/10.1016/j.fuproc.2011.07.004>
- Manjare, S., & Dhingra, K. (2019). Supercritical fluids in separation and purification: A review. *Materials Science for Energy Technologies*, 2(3), 463-484. <https://doi.org/10.1016/j.mset.2019.04.005>

- Moniruzzaman, M., Tahara, Y., Tamura, M., Kamiya, N., & Goto, M. (2010). Ionic liquid-assisted transdermal delivery of sparingly soluble drugs. *Chemical Communications*, 46(9), Article 1452. <https://doi.org/10.1039/b907462g>
- Monti, D., Egiziano, E., Burgalassi, S., Chetoni, P., Chiappe, C., Sanzone, A., & Tampucci, S. (2017). Ionic liquids as potential enhancers for transdermal drug delivery. *International Journal of Pharmaceutics*, 516(1-2), 45-51. <https://doi.org/10.1016/j.ijpharm.2016.11.020>
- Muhammad, N., Elsheikh, Y. A., Mutalib, M. I. A., Bazmi, A. A., Khan, R. A., Khan, H., Rafiq, S., Man, Z., & Khan, I. (2015). An overview of the role of ionic liquids in biodiesel reactions. *Journal of Industrial and Engineering Chemistry*, 21, 1-10. <https://doi.org/10.1016/j.jiec.2014.01.046>
- Painter, P., Veytsman, B., & Youtcheff, J. (2015). Guide to asphaltene solubility. *Energy & Fuels*, 29(5), 2951-2961. <https://doi.org/10.1021/ef502918t>
- Qu, J., Blau, P. J., Dai, S., Luo, H., & Meyer, H. M. (2009). Ionic liquids as novel lubricants and additives for diesel engine applications. *Tribology Letters*, 35(3), 181-189. <https://doi.org/10.1007/s11249-009-9447-1>
- Ramdin, M., de Loos, T. W., & Vlugt, T. J. H. (2012). State-of-the-art of CO₂ capture with ionic liquids. *Industrial & Engineering Chemistry Research*, 51(24), 8149-8177. <https://doi.org/10.1021/ie3003705>
- Rana, M. S., Sámano, V., Ancheyta, J., & Diaz, J. A. I. (2007). A review of recent advances on process technologies for upgrading of heavy oils and residua. *Fuel*, 86(9), 1216-1231. <https://doi.org/10.1016/j.fuel.2006.08.004>
- Salehizadeh, H., Mousavi, M., Hatamipour, S., & Kermanshahi, K. (2007). Microbial demetallization of crude oil using *Aspergillus* sp.: Vanadium oxide octaethyl porphyrin (VOOEP) as a model of metallic petroporphyrins. *Iranian Journal of Biotechnology*, 5(4), 226-231.
- Santos, R. G., Loh, W., Bannwart, A. C., & Trevisan, O. V. (2014). An overview of heavy oil properties and its recovery and transportation methods. *Brazilian Journal of Chemical Engineering*, 31(3), 571-590. <https://doi.org/10.1590/0104-6632.20140313s00001853>
- Selvi, A., Rajasekar, A., Theerthagiri, J., Ananthaselvam, A., Sathishkumar, K., Madhavan, J., & Rahman, P. K. S. M. (2019). Integrated remediation processes toward heavy metal removal/recovery from various environments - A review. *Frontiers in Environmental Science*, 7, 1-15. <https://doi.org/10.3389/fenvs.2019.00066>
- Siriwardana, A. I. (2015). Industrial applications of ionic liquids. In A. A. J. Torriero (Ed.), *Electrochemistry in Ionic Liquids* (pp. 563-603). Springer International Publishing. https://doi.org/10.1007/978-3-319-15132-8_20
- Sowmiah, S., Srinivasadesikan, V., Tseng, M. C., & Chu, Y. H. (2009). On the chemical stabilities of ionic liquids. *Molecules*, 14(9), 3780-3813. <https://doi.org/10.3390/molecules14093780>
- Sun, X., Luo, H., & Dai, S. (2012). Ionic liquids-based extraction: A promising strategy for the advanced nuclear fuel cycle. *Chemical Reviews*, 112(4), 2100-2128. <https://doi.org/10.1021/cr200193x>
- Tavakoli, O., & Yoshida, H. (2005). Effective recovery of harmful metal ions from squid wastes using subcritical and supercritical water treatments. *Environmental Science & Technology*, 39(7), 2357-2363. <https://doi.org/10.1021/es030713s>

- Trucillo, P., Campardelli, R., Scognamiglio, M., & Reverchon, E. (2019). Control of liposomes diameter at micrometric and nanometric level using a supercritical assisted technique. *Journal of CO₂ Utilization*, 32, 119-127. <https://doi.org/10.1016/j.jcou.2019.04.014>
- Vancov, T., Alston, A. S., Brown, T., & McIntosh, S. (2012). Use of ionic liquids in converting lignocellulosic material to biofuels. *Renewable Energy*, 45, 1-6. <https://doi.org/10.1016/j.renene.2012.02.033>
- Visser, A. E., Swatloski, R. P., Reichert, W. M., Davis Jr., J. H., Rogers, R. D., Mayton, R., Sheff, S., & Wierzbicki, A. (2001). Task-specific ionic liquids for the extraction of metal ions from aqueous solutions. *Chemical Communications*, 1, 135-136. <https://doi.org/10.1039/b0080411>
- Wang, S., Xu, X., Yang, J., & Gao, J. (2011). Effect of the carboxymethyl chitosan on removal of nickel and vanadium from crude oil in the presence of microwave irradiation. *Fuel Processing Technology*, 92(3), 486-492. <https://doi.org/10.1016/j.fuproc.2010.11.001>
- Welter, K., Salazar, E., Balladores, Y., Márquez, O. P., Márquez, J., & Martínez, Y. (2009). Electrochemical removal of metals from crude oil samples. *Fuel Processing Technology*, 90(2), 212-221. <https://doi.org/10.1016/j.fuproc.2008.09.004>
- Yuan, J., Yang, Y., Zhou, X., Ge, Y., & Zeng, Q. (2019). A new method for simultaneous removal of heavy metals and harmful organics from rape seed meal from metal-contaminated farmland. *Separation and Purification Technology*, 210, 1001-1007. <https://doi.org/10.1016/j.seppur.2018.09.056>
- Zhao, X., Xu, C., & Shi, Q. (2015). Porphyrins in heavy petroleums: A review. In C. Xu & Q. Shi (Eds.), *Structure and Modeling of Complex Petroleum Mixtures* (Vol. 168: pp. 39-70). Springer International Publishing. https://doi.org/10.1007/430_2015_189